Electronic Supplementary Material (ESI) for Journal of Materials Chemistry A.

Supporting Information

Bismuth Nanodendrites as High Performance Electrocatalysts for Selective Conversion of CO_2 to Formate

Hexiang Zhong [a,b*], *Yanling Qiu*[a], *Taotao Zhang*[a,c], *Xianfeng Li* [a,b], *Huamin Zhang* [a,b*] , *Xiaobo Chen*[d]

[a] Division of Energy Storage, Dalian National Laboratory for Clean Energy (DNL), Dalian Institute of Chemical Physics, Chinese Academy of Sciences, Dalian 116023, China.

[b] Collaborative Innovation Center of Chemistry for Energy Materials (iChEM), Dalian 116023 (P.R. China).

[c] University of the Chinese Academy of Sciences, Beijing 100049, China.

[d] Department of Chemistry, University of Missouri, Kansas City 64110, USA.

* Correspondence to: zhonghexiang@dicp.ac.cn; zhanghm@dicp.ac.cn;

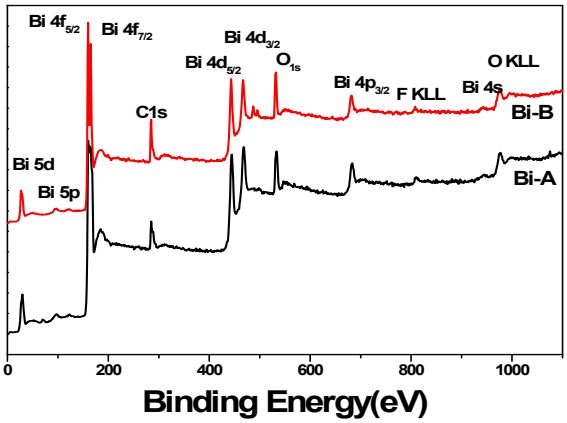

Fig. S1 shows XPS survey spectra for the Bi catalysts over a wide range of binding energies from 000 eV to 1100 eV.

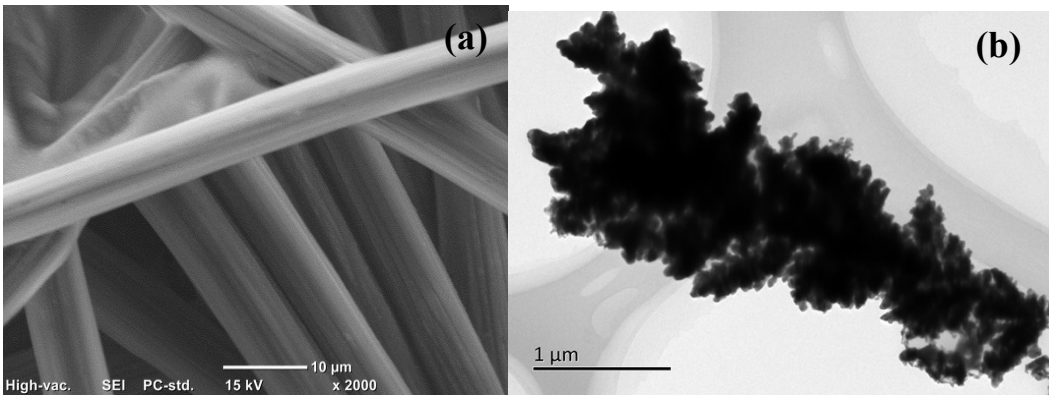

Fig. S2 (a) SEM images for treated carbon paper (b) TEM images for Bi-B catalysts

Fig. S2a shows the SEM images for carbon paper. It can be observed the treated carbon paper（TCP） comprises of nanofibers and the surface of the TCP is very smooth. Fig. S2b displays the TEM images for Bi-B catalysts. From the TEM images, the Bi-B presents nanodendrties structures.

To clarify the Bi-B nanodendrites formation process, SEM images for Bi-B catalysts synthesized with different amount of KBr and different growth durations were collected. Figure S3 shows the SEM images for Bi-B catalysts synthesized with different amount of KBr from 0.01 M -0.5 M. As shown in Figure S3, with the addition of small amount of KBr during the electrochemical deposition process, Bi nanoparticles with foam-like, spherical morphology can be obtained, which is significantly different with structure of Bi-A composed of the irregular pellet. With increase of the KBr amount, the Bi branches appear on the surface of the nanoparticles. When the KBr amount increases to 0.2 M, the dendrites with short branches have been formed. This demonstrates the Br^- can act as capping agent, which can facilitate the formation of small size of spherical nanoparticles. The selective adsorption of the Br^-, the orientated growth occurs, which leads to the formation of larger size branches and nanodendrites.

Figure S4 shows the SEM images for Bi-B catalysts synthesized at -0.35 V for different

time (a,b) 50s; (c,d) 100s (e,f) 200s (g,h) 400s (j,k) 600s. It can be observed that the Bi-B synthesized at -0.35V for 50s, the nanowire can be formed with small particle size. With the increase the deposition time, the nanodendrites can be formed. Moreover, the size of the nanodendrites and their branches become larger with the deposition time changes from 200s to 600s.

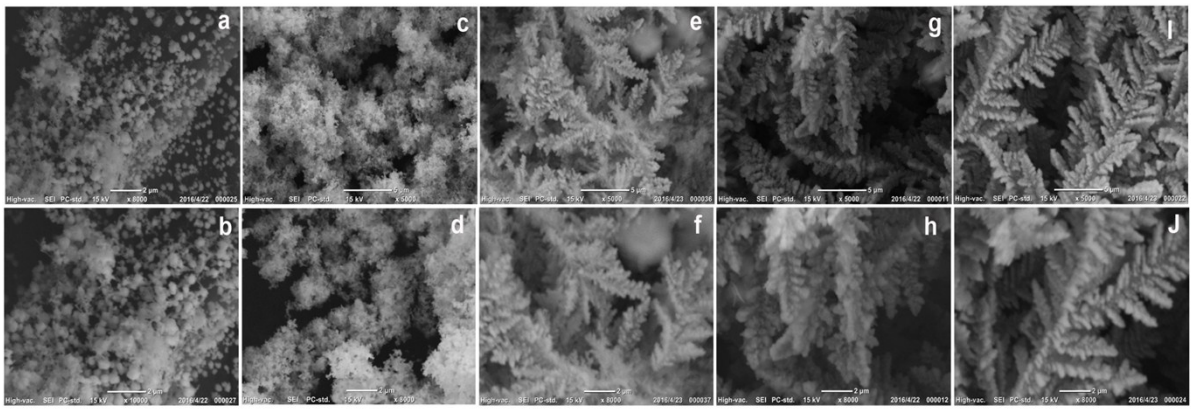

Figure S3 (a) SEM images for Bi-B catalysts synthesized with different amount of KBr (a,b) 0.01 M (c,d) 0.05 M (e,f) 0.2 M (g,h) 0.3 M (I,J) 0.5 M

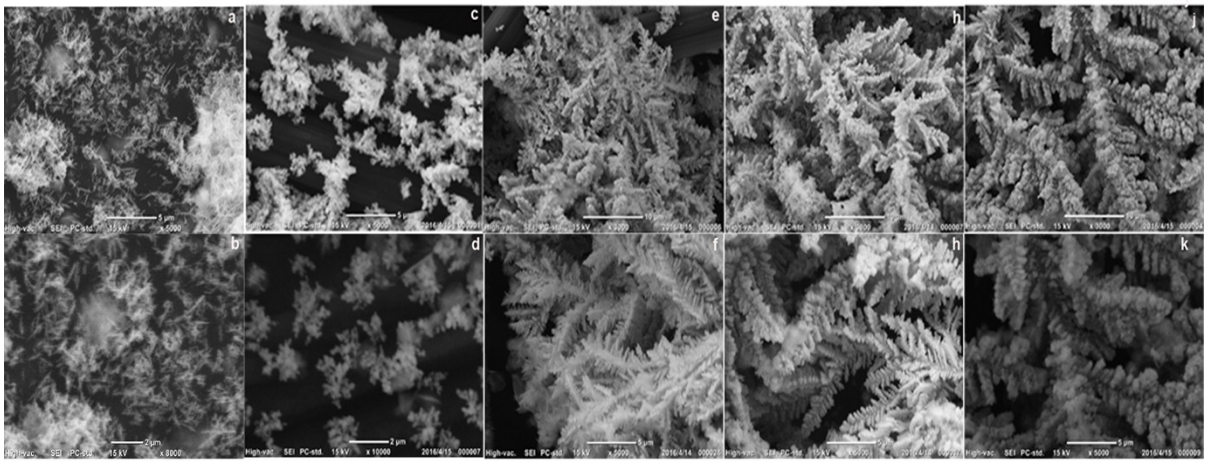

Figure S4 (a) SEM images for Bi-B catalysts synthesized at -0.35 V for different time (a,b) 50s; (c,d) 100s (e,f) 200s (g,h) 400s (j,k) 600s

Cyclic voltammetry (CV) was performed in the three-electrode system with the N_2 saturated 0.5 M $NaHCO_3$ as electrolyte. CVs were obtained for a potential range in which no

faradaic processes were occurring, and the geometric current density was plotted against the scan rate of the CV[1,2].

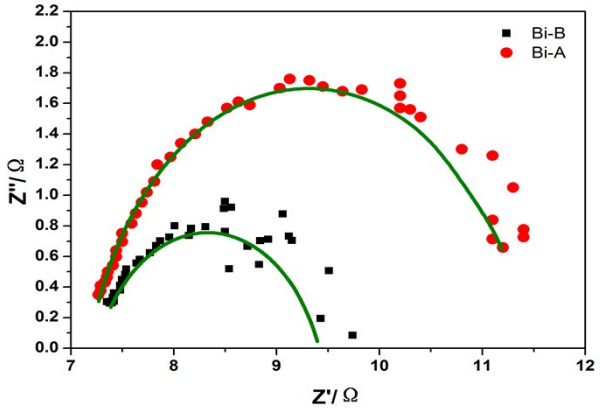

Figure S5. Niquist impedance spectra for different catalysts at the applied potential of -1.8 V vs. SCE.

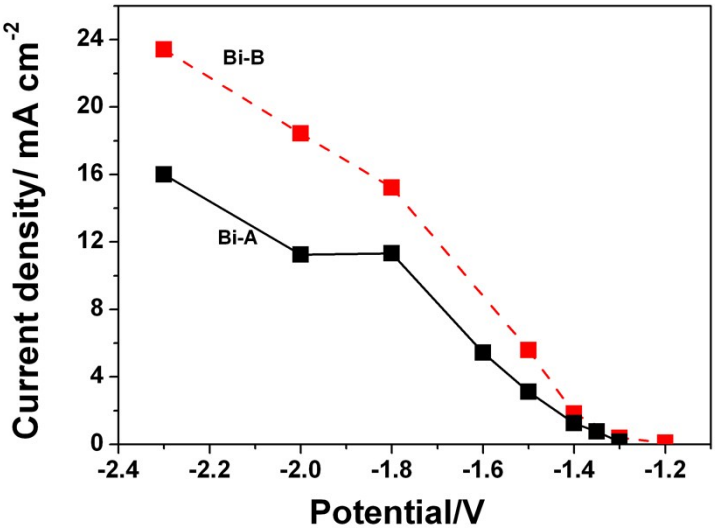

Figure S6. Applied electrolysis potentials vs. partial current densities for $HCOO^-$ production on Bi-A and Bi-B, 0.5 M $NaHCO_3$.

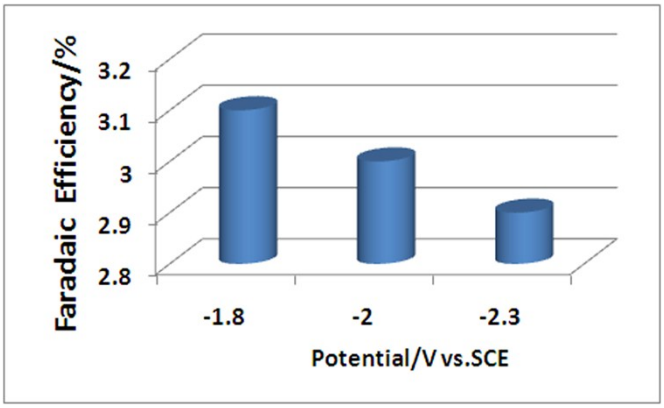

Figure S7. FEs for $HCOO^-$ production of carbon paper at various potentials in 0.5 M $NaHCO_3$, pH 7.2.

The stability was evaluated at -1.8 V for 10 h and 50 h, respectively. During the test, the current-time curves were recorded. Before and after the test, the $HCOO^-$ concentrations were measured respectively.

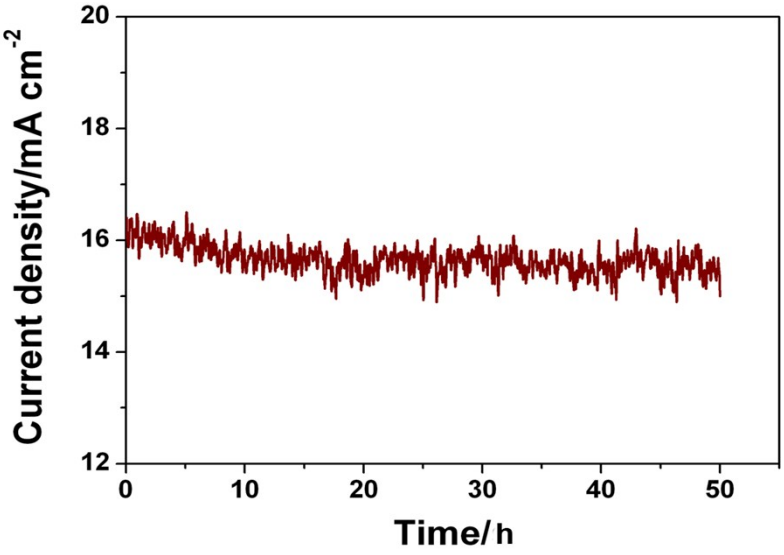

Figure S8. Total current density vs time for $HCOO^-$ production on Bi-B/TCP electrode

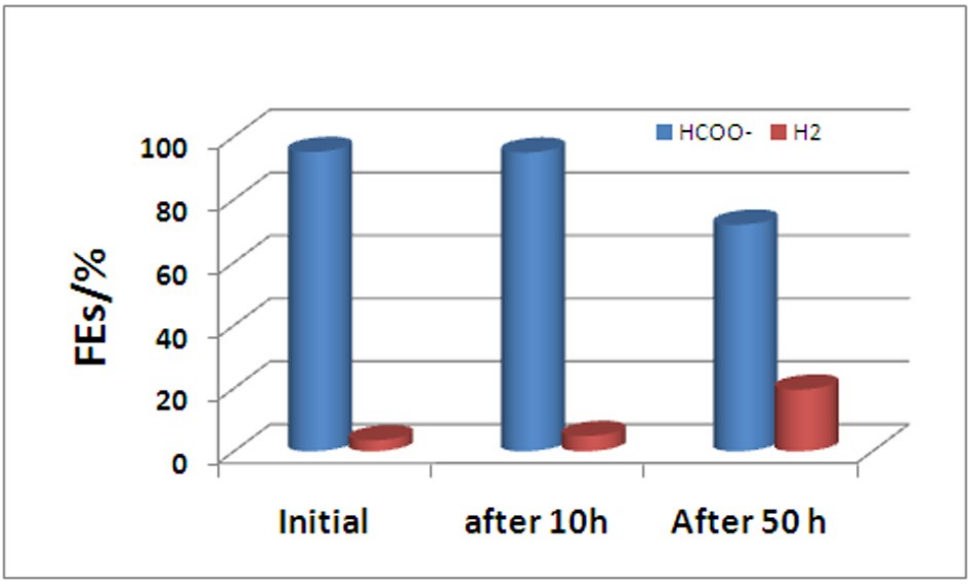

Figure S9. Initial FE and FE after 10 h and 50 h for $HCOO^-$ and H_2 production on Bi-B/TCP electrode

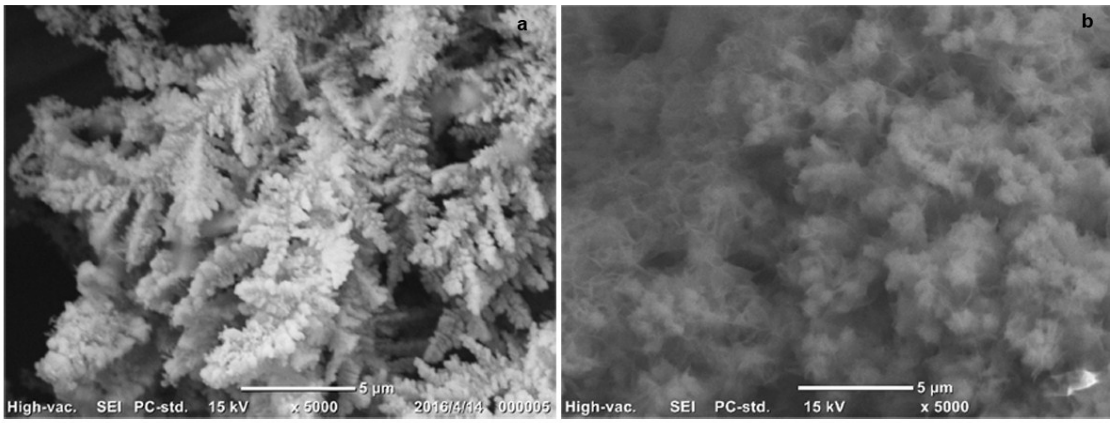

Figure S10 SEM images after 10 h and 50 h continuous electrolysis on Bi-B/TCP electrode

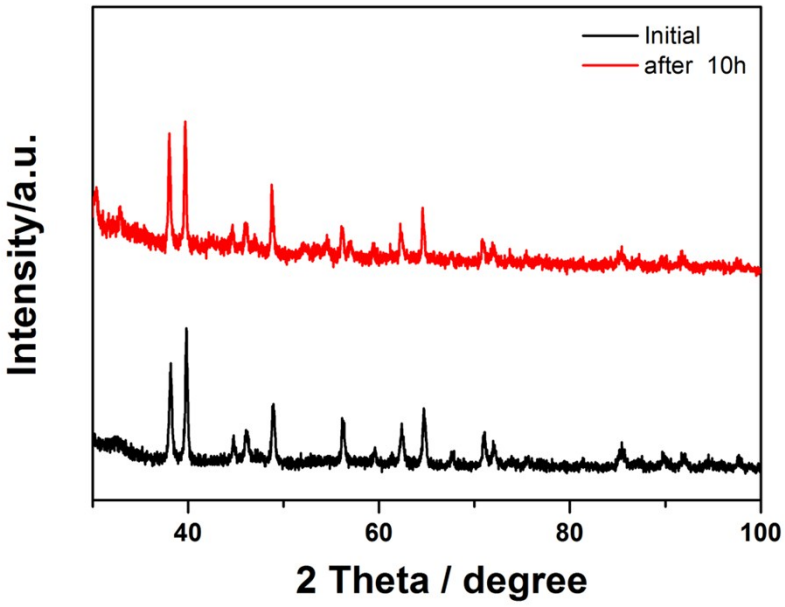

Figure S11 XRD after 10 h continuous electrolysis on Bi-B/TCP electrode

Table S1 Comparison of ERC performance for Bi-B and recent reported non-heavy metal electrocatalysts for CO_2 reduction to formate

Catalyst/ electrodes	**Electrolyte**	**Potential/V vs. SHE**	**J $_{HCOO^-}$ (mA cm^{-2})**	**FEs %**	**Ref.**
Bi –B	**0.5 M $NaHCO_3$**	**-1.558**	**15.2**	**96**	**This work**
Ir Pincer /CNT	0.5m $LiClO_4$+ 0.1 M $NaHCO_3$, 1% v/v MeCN,	-1.4	15.2	83	Angew. Chem. Int. Ed. 2014, 53, 8709.
Sn-loading GDE	0.5 M $KHCO_3$	-1.59	17.43	78.6	J. Power Sources 2014 271, 278.
Polyethylenimine -NCNT	0.1 M $KHCO_3$	-1.558	9.5	87	J. Am. Chem. Soc. 2014, 136, 7845.
$Pd_{70}Pt_{30}$/C catalyst	0.1M KH_2PO_4/0.1 M K_2HPO_4)	-0.4 V vs RHE	5	88.0	Acs Catalysis 2015, 5 , 3916.
Pb	Na_2SO_4, H_2SO_4	----	0.115	97	J. Appl. Electrochem. 1987,17, 159.
[Cu(cyclam)](ClO_4)$_2$ complex	DMF/H_2O (97/3 v/v)	-2.0 V vs. Fc+/Fc	1.3	90	J. Mater. Chem. A, 2015, 3, 3901–3907
Sn/SnO_x, composite	0.5 M $NaHCO_3$	-0.7 V RHE	< 5	58	J. Am. Chem. Soc. 2012, 134, 1986

Reference

1. C.W. Li, M.W. Kanan, J. Am. Chem. Soc. 2012, 134, 7231.

2. D. Raciti, K. J. Livi, C. Wang, Nano Lett. , 2015, 15, 6829.